Journal of Physics: Condensed Matter

PAPER

Two-dimensional conducting states in infinite-layer oxide/perovskite oxide hetero-structures

To cite this article: Xiaobing Chen *et al* 2022 *J. Phys.: Condens. Matter* **34** 035003

IOP Publishing

Journal of Physics: Condensed Matter

J. Phys.: Condens. Matter **34** (2022) 035003 (7pp)

https://doi.org/10.1088/1361-648X/ac30b6

Two-dimensional conducting states in infinite-layer oxide/perovskite oxide hetero-structures

Xiaobing Chen[1,2], **Jine Zhang**[3], **Banggui Liu**[1,2], **Fengxia Hu**[1,2,4], **Baogen Shen**[1,2,4] and **Jirong Sun**[1,2,4,5,*]

[1] Beijing National Laboratory for Condensed Matter Physics & Institute of Physics, Chinese Academy of Sciences, Beijing 100190, People's Republic of China
[2] School of Physical Sciences, University of Chinese Academy of Sciences, Beijing 100049, People's Republic of China
[3] School of Integrated Circuit Science and Engineering, Beihang University, Beijing 100191, People's Republic of China
[4] Songshan Lake Materials Laboratory, Dongguan, Guangdong 523808, People's Republic of China
[5] Spintronics Institute, University of Jinan, Jinan, Shandong 250022, People's Republic of China

E-mail: jrsun@iphy.ac.cn

Received 26 August 2021, revised 9 October 2021
Accepted for publication 18 October 2021
Published 3 November 2021

Abstract

Heterointerfaces sandwiched by oxides of dissimilar crystal structures will show strong interface reconstruction, leading to distinct interfacial effect arising from unusual physics. Here, we present a theoretical investigation on the interfaces between infinite-layer oxide and perovskite oxide ($SrCuO_2/SrTiO_3$ and $SrCuO_2/KTaO_3$). Surprisingly, we found well-defined two-dimensional electron gas (2DEG), stemming from atomic reconstruction and polar discontinuity at interface. Moreover, the 2DEG resides in both the TiO_2 and CuO_2 interfacial layers, unlike $LaAlO_3/SrTiO_3$ for which 2DEG exists only in the TiO_2 interfacial layer. More than that, no metal-to-insulator transition is observed as the $SrCuO_2$ layer thickness decreases to one unit cell, i.e., the metallicity of the new interface is robust. Further investigations show more unique features of the 2DEG. Due to the absence of apical oxygen at the $SrCuO_2/SrTiO_3$ ($KTaO_3$) interface, the conducting states in the interface TiO_2 (TaO_2) layer follows the $d_{xy} < d_{3z^2-r^2} < d_{xz/yz}$ orbital order rather than the $d_{xy} < d_{xz/yz}$ orbital order of paradigm $LaAlO_3/SrTiO_3$ ($KTaO_3$), exhibiting enhanced interfacial conduction. This work suggests the great potential of heterointerfaces composed of non-isostructural oxides for fundamental research.

Keywords: complex oxide interface, two dimensional electron gas, density functional calculations, nonisostructural interface

S Supplementary material for this article is available online

(Some figures may appear in colour only in the online journal)

---

[*] Author to whom any correspondence should be addressed.

1. Introduction

Heterointerfaces of complex transition-metal oxides offer a good platform for manipulating the charge, spin, orbital and lattice degrees of freedom to generate diverse phenomena with abundant physics [1, 2]. A prominent example is the two-dimensional electron gas (2DEG) residing in interfacial layer between two perovskite oxide insulators, $LaAlO_3$ (LAO) and $SrTiO_3$ (STO) [3]. When they are joined at heterointerface, polar discontinuity would lead to a charge accumulation at the $(LaO)^{1+}/(TiO_2)^{1-}$ interface, making the interfacial layer *n*-type doped when the LAO layer reaches a critical thickness of 4 *uc* [4, 5]. Compared with conventional semiconductor 2DEG [6], the 2DEG at oxide interfaces exhibits a wider spectrum of exotic effects including macroscopic quantum effect [7], non-reciprocal charge transport [8], interface superconductivity [9] and magnetism [10] have been observed.

Most of previous investigations focused on 2DEGs between two perovskite oxide insulators. Non-isostructural complex oxide interfaces have attracted considerable interest for both fundamental physics and potential applications due to the enhanced interface reconstructions, resulting in unexpected effects. As reported, 2DEG exhibits an extremely high Hall mobility when formed at γ-Al_2O_3/STO interface [11] and visible spin polarization when sandwiched between EuO and $KTaO_3$ (KTO) [12].

Generally, it is believed that the polar discontinuity at interface play an important role in the emergence of 2DEG [4]. Therefore, grouping oxides with strong electric polarity with non-polar STO is a natural way toward novel 2DEG. Infinite-layer oxides ANiO$_2$ (A = La, Nd, Pr, etc) has high polarity mismatch to STO (+3/0 for $(A)^{3+}/(TiO_2)^0$ interface). However, as ANiO$_2$ is a bad metal, the Ni valence can change to partially screen the polar discontinuity at interface, depressing 2DEG [13, 14].

Here, we pursue a new route to achieve 2DEG by employing an infinite-layer cuprate $SrCuO_2$ (SCO) as the top layer, which possesses alternative polar planes of $(Sr)^{2+}$ and $(CuO_2)^{2-}$ along the [001] direction. As a polar oxide, SCO is a charge-transfer insulator with a band gap of 1.5 eV [15], much narrower than that of LAO (5.6 eV) [4]. Besides, SCO owns the lattice parameters of $a = 3.926$ Å and $c = 3.432$ Å and is subject to slightly compressive strain (+0.54%) when epitaxially grown on STO (001) [16]. This small lattice mismatch ensures the epitaxial growth of SCO on STO. Compared to the mostly investigated LAO/STO system, the SCO/STO system has smaller lattice mismatch, higher polarity mismatch and stronger interfacial reconstructions. The interface between the SCO and the polar typical substrate $KTaO_3$ (KTO) was also investigated for comparison, where SCO suffered tensile strain of −1.58%.

In both heterostructures we observed 2DEG. Here, we shed light on the nature of the electronic structure at the symmetry-breaking interface and surface. Based on the calculated plane-averaged electrostatic potential and strong polar-like displacements, we believed that interface conducting states originated from the electronic reconstruction driven by polar discontinuity at interface. The internal electric field in the SCO region and the polar-catastrophe-induced charge transfer are estimated, confirming that the strong lattice polarization compensated the dipolar electric field. Different from $LaAlO_3$, SCO is a small-band-gap semiconductor. The electric field cannot be sustained by band gap, thus the 2DEG emerges at any thickness of SCO film, i.e., no critical thickness is necessary for triggering metallic states at interface. Moreover, as the built-in electric field is bigger than the band gap of SCO, the interfacial CuO_2 layer also adopted an electron-doping state. As a consequence, the interfacial layers are conducting not only for STO (KTO) but also for SCO. Furthermore, distinct from conducting states with the t_{2g} orbital character in LAO/STO (KTO) system, we found that the orbital level splitting at the interfaces was strongly modified by the absence of apical oxygen at interface, resulting in occupation of the interfacial d_{xy} and $d_{3z^2-r^2}$ orbitals for the Ti and Ta atoms. These analyses suggest new 2DEG systems with an enhanced interfacial electron conductivity with respect to the LAO-based 2DEG.

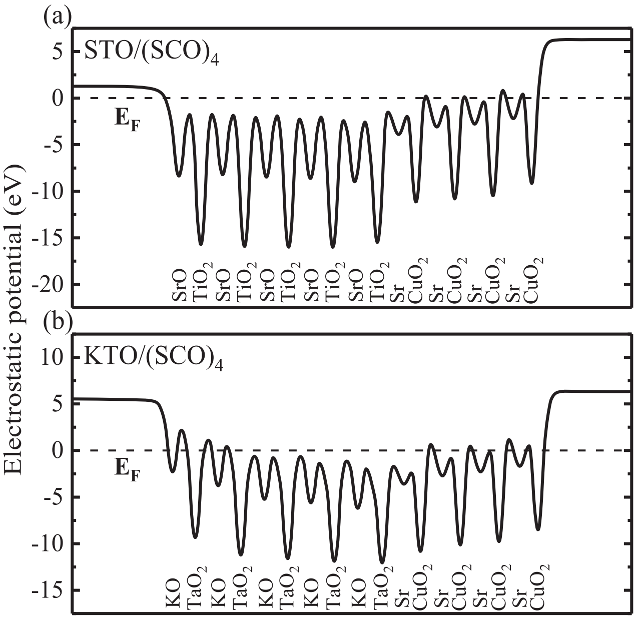

Figure 1. Plane-averaged electrostatic potential for (a) $(SCO)_4$/STO and (b) $(SCO)_4$/KTO heterostructures along the stacking direction.

2. Computation details

We performed the first-principles calculations in the framework of density functional theory (DFT) as implemented in the vienna *ab initio* simulation package codes [17, 18]. The generalized gradient approximation of Perdew–Burke–Ernzernhof modified for solids was adopted for the calculation of exchange–correlation energy [19, 20]. A cutoff energy of 600 eV was found to achieve numerical convergence. We used $13 \times 13 \times 13$ (bulk) and $13 \times 13 \times 1$ (slab) Monkhorst-Pack k-point meshes in the electronic structure calculations [21]. To consider the static correlation effects, the DFT + U approach within the rotationally invariant Dudarev's formalism was performed with $U_{Ti} = 5.0$ eV, $J_{Ti} = 0.64$ eV, $U_{Cu} = 7.5$ eV, $J_{Cu} = 0.98$ eV for Ti and Cu 3d orbitals, respectively [22–24].

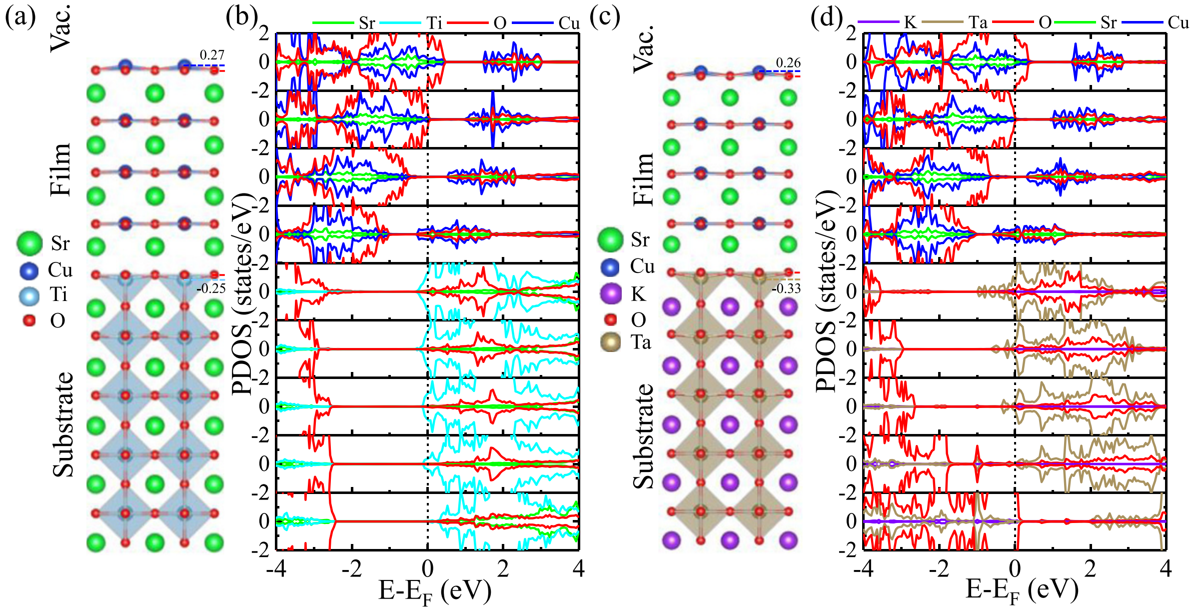

Figure 2. Optimized atomic structure of (a) $(SCO)_4$/STO and (c) $(SCO)_4$/KTO films and the corresponding layer-projected density of states in (b) and (d). The vertical displacements Δz of surface Cu site ions and interfacial Ti/Ta site ions from their respective oxygen layers are also shown in (a) and (c).

The ionic positions were carefully optimized, reducing the Hellman–Feynman force on each atom below 0.01 eV $Å^{-1}$. The electronic iteration was performed until the total energy change was smaller than 10^{-5} eV. Convergence tests about the computational details are shown in supplemental materials (https://stacks.iop.org/JPCM/34/035003/mmedia) [25].

We modeled the Sr/TiO_2 terminated SCO/STO (001) and Sr/TaO_2 terminated SCO/KTO (001) in film geometry by using the $\sqrt{2}a \times \sqrt{2}a$ supercells biaxially strained to $a = 3.905$ Å and $a = 3.989$ Å, which are the lattice parameters of bulk STO and KTO substrate, respectively. The slabs contained five STO (KTO) unit cells and m unit cells SCO ($m = 1$–6). The vacuum region spans 20 Å to prohibit the out-of-plane electronic interactions between neighboring heterostructures and the dipole correction was always applied to remove artificial dipole interaction [26]. All the atoms were fully relaxed except for the lowest two STO (KTO) unit cells which were fixed to simulate substrate effects. The bulk properties of the parent compounds SCO, STO and KTO can be obtained from supplemental materials [25], including experimental and DFT equilibrium lattice parameters and band gaps.

3. Results and discussion

3.1. Polar discontinuity at interface

SCO films grown on a BO_2-terminated ABO_3 (001) substrate can be viewed as an alternately stacking of the polar $(Sr)^{2+}$ and $(CuO_2)^{2-}$ planes. In this vein, the local ionic dipole moment arouses inevitably a built-in electric field in the SCO layers of the heterostructures. In order to clearly illustrate how the polar field modifies electronic structure, we show in figures 1(a) and (b) the plane-averaged electrostatic potential along the z direction perpendicular to the interface/surface of the $(SCO)_4$/STO (KTO) heterostructure.

For the SCO/STO system, the trend of electrostatic potential on the STO side is almost flat, indicating the absence of obvious internal electric field within STO, i.e., STO is a nonpolar oxide. In the SCO part, there exists an ascendant slope from the interface to the surface for the electrostatic potential. As a result, the electron is unavoidably transferred to the interfacial TiO_2 layer, forming 2DEG. For the SCO/KTO system, however, not only SCO but also KTO donate electrons to interfacial TaO_2 layer. Similar results are obtained as the thickness of SCO varies from $m = 1$ to 6 [25]. Therefore, the two-dimensional conducting states are robust in the adopted models for $(SCO)_m$/STO and $(SCO)_m$/KTO.

3.2. Density of states of the heterostructures

To understand the origin of the conducting states and the associated charge transfer in the SCO/STO and SCO/KTO heterostructures, the corresponding layer-projected density of states (PDOS) are computed as shown in figure 2. From figures 2(a) and (c), polar-like Ti/Ta displacement can be clearly seen at interface, which is the typical feature of 2DEG at complex oxide interface. As shown in figures 2(b) and (d), the Fermi level crosses the conduction band minimum at both CuO_2 and TiO_2 (TaO_2) interfacial layers, indicating n-type interfacial conductivity. Moreover, it crosses the valence band maximum at the surface of CuO_2 layer, implying the appearance of p-type conducting state on surface. The DOS in the central part of SCO compares well with that of the bulk [25], indicating that the SCO-based conducting states are two dimensional.

As we all know, in octahedral crystal field, the five d orbitals are splitting into three lower t_{2g} orbitals and two

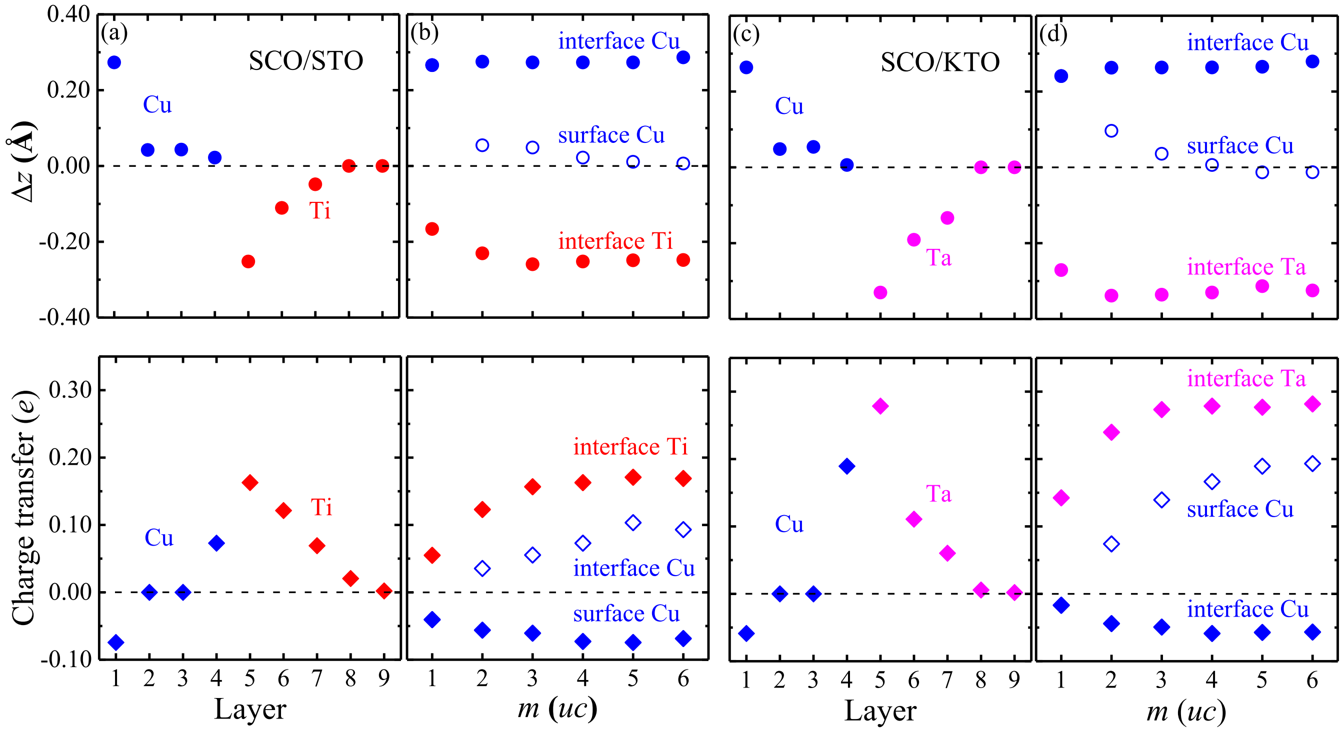

Figure 3. Atomic displacements along out-of-plane direction and charge transfer for (a) SCO/STO and (c) SCO/KTO heterostructures, presented as functions of layer position. Obvious ionic shift takes place in interfacial layers, implying the occurrence of lattice polarization. (b) and (d) Atomic displacements and charge transfer as functions of the layer thickness of SCO.

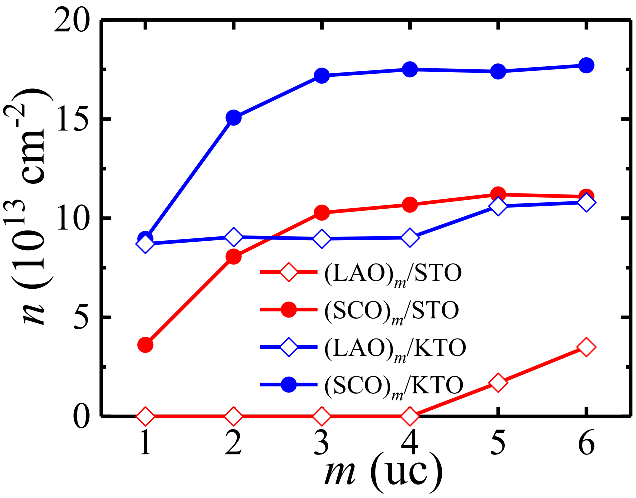

Figure 4. Interfacial carrier density as a function of top layer thickness for SCO-based and LAO-based 2DEGs. The calculated interfacial carrier density of LAO-based 2DEG is derived from Wang's work [33].

higher e_g orbitals (For Ti and Ta are $3d$, $5d$ orbitals, respectively). Because of inversion symmetry breaking along [001] direction, three t_{2g} orbitals further split into two higher $d_{xz/yz}$ orbitals and a lower d_{xy} orbital [27, 28]. In heterostructures, the TiO$_6$ octahedron at $(\mathrm{Sr})^{2+}/(\mathrm{TiO}_2)^0$ interface is replaced by a TiO$_5$ square pyramid due to the missing of the apical oxygen. Therefore, the $d_{3z^2-r^2}$ orbital is significantly lowered, it can be occupied and contributes nearly half metallic states at the interfacial TiO$_2$ layer as calculated from the orbital-resolved PDOS in figure 5(a). In other words, the metallic states at the interfacial TiO$_2$ layer are contributed by Ti $d_{3z^2-r^2}$, d_{xy} and $d_{xz/yz}$ orbitals. This is different from LAO/STO 2DEG, for which the conducting state are made of primarily d_{xy} orbital [27, 28]. As for the SCO/KTO system, the metallic states at the interfacial TaO$_2$ layer originate from Ta d_{xy} and $d_{3z^2-r^2}$ orbitals.

3.3. Atomic reconstruction and charge transfer

To reveal the atomic and electronic reconstruction at new interface and their effect on electronic structure, we calculated layer-resolved vertical polar-like displacements of the B site ions (B = Ti/Ta, Cu), with respect to oxygen layers, and layer-resolved charge transfer at B sites. The results are shown in figure 3(a) for SCO/STO and 3(c) for SCO/KTO system. Meanwhile, the B site ionic displacements and charge transfer are also presented as functions of film thickness (figures 3(b) and (d)). Based on the DFT calculations, for SCO/STO system with $m = 4$, the surface Cu lost 0.08 e$^-$, while the interfacial Ti and Cu gain 0.17 and 0.07 e$^-$, respectively. For (SCO)$_4$/KTO, we observe similar charge transfer: the surface Cu lost 0.06 e$^-$, while the interfacial Ta and Cu gain 0.28 and 0.19 e$^-$, respectively. As the film thickness increases from four to six unit cells, only negligible changes in charge transfer are observed, suggesting the applicability of our model to thick films.

One thing deserves special attention is that the number of the transferred charges are much smaller than that deduced from the polar catastrophe model. According to the electrostatic analysis of polar discontinuity at surface, atomic reconstruction should provide 1.0 e$^-$ per unit cell at the

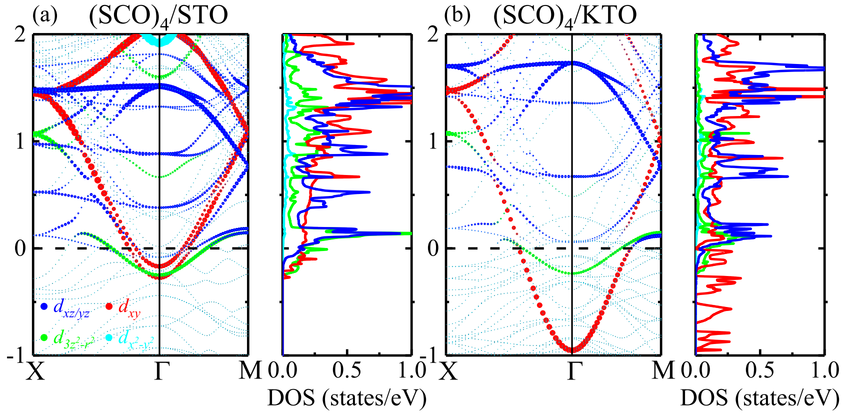

Figure 5. Orbital-projected band structure and corresponding PDOS of (a) interfacial Ti 3*d* in SCO/STO and (b) interfacial Ta 5*d* in SCO/KTO heterostructures. The size of the red, green and blue dots represents the weight of Ti (Ta)–d_{xy}, $d_{3z^2-r^2}$, $d_{xz/yz}$ orbitals, respectively. The $d_{x^2-y^2}$ orbitals are not shown here as they located far away from Fermi level.

(Sr)$^{2+}$/(TiO$_2$)^0 interface to fully compensate the internal electric field in the SCO/STO heterostructures. For the SCO/KTO heterostructures, 1.5 e$^-$ per unit cell should be transferred to interfacial Ta, including 1.0 e$^-$ from SCO and 0.5 e$^-$ from KTO side. We use a simple parallel-plate capacitor model [4, 29, 30] to explain this discrepancy.

Take the SCO/STO system with $m = 4$ as an example. The internal electric field is $E = 0.23$ V Å^{-1} in SCO, derived from the potential slope in figure 1(a). Thus, the electrostatic potential drop [31] from the surface to the interface SCO layer is $\Delta V = emcE \sim 3.1$ eV, here c stands for the out-of-plane lattice constants of SCO. Such a large ΔV cannot be sustained by the narrow band gap of SCO (1.5 eV from experiments or 0.9 eV from DFT calculations). As a result, a two-dimensional hole gas appears in the top CuO$_2$ surface and a 2DEG develops in the interfacial CuO$_2$ layer as implied by figure 2(b). In this case, we can estimate the number of transferred electrons to interface adopting $n = \frac{\varepsilon_r a^2 E}{4\pi mc}$, where ε_r is the dielectric constant of bulk SCO, a is the in-plane lattice constants. Setting ε_r to 8 according to Zhong *et al* [32], we obtained a charge transfer of $n = 0.28$ e$^-$, consistent with 0.25 e$^-$ (0.17 + 0.08 e$^-$) as calculated from layer PDOS in figure 2(b).

According to DFT calculations, on the other hand, the interfacial Ti (Ta) displays a polar-like displacement of -0.25 Å (-0.33 Å) as denoted in figure 2(a) (2(c)). This displacement is larger than that for bare STO and KTO film (about -0.08 Å). This polar-like displacement neutralizes the polar-discontinuity-induced charge transfer. As a consequence, only a small number of electrons are transferred to interfacial layer. We can estimate the interfacial carrier density from the displacements of Sr and CuO$_2$ layer adopting $n = \frac{\varepsilon_r a^2 \Delta V}{4\pi e \sum Z_i \Delta z_i} \sim 0.20$ e$^-$, which is consistent with 0.25 e$^-$, here Z_i denotes the nominal charges of Sr or Cu, z_i represents the displacements of Sr or Cu. These two rough estimations imply that the internal electric field arising from the surface dipole moment is screened by electronic and ionic polarization, explaining why the charge transfer is much less than the expected value of 1.0 e$^-$.

There are two unique features for the SCO-based 2DEG compared with LAO/STO system. The first one is the absence of a threshold thickness for the top layer to form 2DEG, which shows the intrinsically conducting in our 2DEG, and second one is the much higher carrier density of the 2DEG. To have a qualitative comparison, we plot the interfacial charge density as a function of the number of the SCO or LAO unit cells, obtained by integrating the PDOS of the occupied Ti 3*d* (Ta 5*d*) orbitals of the interfacial TiO$_2$ (TaO$_2$) layer. As shown in figure 4, for the SCO-based 2DEG, the calculated carrier density is in the order of 10^{14} cm^{-2}, which is three times larger than that in the corresponding LAO-based 2DEG with the same substrate and film thickness. Therefore, using SCO as the top layer will improve conductivity of the 2DEG.

3.4. Band structures

According to the orbital-resolved PDOS in figure 5, the SCO-based 2DEG hosts multiple conducting states associated with different orbitals of the interfacial Ti (Ta) atoms. In figure 5, we plot the band structures of the SCO-based heterostructures. Take the SCO/STO heterostructure as an example. It is clear that the conduction bands are filled with many bands, resulting in a two-dimensional electron gas. The occupied Ti d_{xy} orbitals (-0.28 eV) and $d_{3z^2-r^2}$ orbitals (-0.25 eV) give rises to conducting states centered around the Γ point, whereas the $d_{xz/yz}$ orbitals lead to the metallic states located a little far away from the Γ point. Meanwhile, the Cu $d_{x^2-y^2}$ orbitals located around the *X* point also contribute to interfacial metallic states as shown in figure S6 [25].

To qualitatively compare the electron transport property with LAO/STO, the electron effective mass of the bottom conduction band is further calculated. It is $m^*/m_e = 0.49$ for the Ti d_{xy} orbitals, obtained by using parabolic approximation along the Γ–*X* direction. It inherits the intrinsic feature of Ti d_{xy} orbital in the parent bulk material STO [28, 34, 35]. The electron effective mass is 1.02 for the Ti $d_{3z^2-r^2}$ orbital. For the SCO/KTO heterostructures, the calculated m^*/m_e is 0.33 for the Ta d_{xy} (-0.95 eV) along the Γ–*X* direction, which is much lower than that of the Ti d_{xy} orbitals. This is due to the less localization of the Ta 5*d* orbitals than Ti 3*d* orbitals. The electron effective mass of Ta $d_{3z^2-r^2}$ (−0.24 eV) is 1.09. We note that the $d_{3z^2-r^2}$ orbitals of Ti and Ta possess similar values regardless of their own orbital feature, which can be ascribed to their hybridization with Cu $d_{3z^2-r^2}$ orbital. Notably, the d_{xy} and $d_{3z^2-r^2}$ orbitals contributed about 33% and 41% to the interfacial Ti metallic states in SCO/STO heterostructures, while they contributed about 78% and 13% to the interfacial Ta metallic states in SCO/KTO heterostructures. We attribute this difference to the different orbital splitting energy between t_{2g} and e_g. As shown in figure 5, the Ta d_{xy} locates well below the $d_{3z^2-r^2}$ orbitals, probably due to the higher oxidization state and larger atomic number that Ta has [36]. Moreover, this orbital order manipulation in SCO-based 2DEG not only tune the electronic properties as stated before, but also should affect the Lifshitz transition [37] and superconductivity [38]. Our findings provide a new perspective to manipulate the orbital order through interface design by structural symmetry mismatch.

4. Conclusion

Based on first-principles calculations, we predicted presence of polar-discontinuity-induced 2DEGs in stoichiometric SCO/STO (SCO/KTO) hetero-structures. Key factors affecting 2DEG are discovered, including polar-like ionic displacements at interface, band bending and the charge transferring to interface, the latter leads to a 2DEG residing in both TiO_2 (TaO_2) and CuO_2 interface layers and a two-dimensional hole gas on the surface of the CuO_2 layer. Further investigation reveals more unique feature of the 2DEG. Surprisingly, one-unit-cell-thick SCO layer is enough to generate 2DEG, i.e., the metallic interface is robust. Different from the paradigm LAO/STO (LAO/KTO) system, the orbital ordering of the mobile electrons at interfacial TiO_2 (TaO_2) layer is further manipulated where the $d_{3z^2-r^2}$ band shifts below the Fermi level and thus populates, resulting in an enhanced interfacial carrier density generally in the order of 10^{14} cm^{-2}. This is much higher than that of the LAO/STO 2DEG but lower than the expected value generated by polar catastrophe. The strong polar-like displacements of Ti or Ta sites at interface significantly compensate the built-in electric field at interface, depressing charge transfer. Our investigation provides new insights into different interfacial properties and the primary mechanism responsible for the formation of 2DEGs between infinite-layer polar small-band-gap insulator SCO and conventional STO and KTO substrate.

Acknowledgments

This work has been supported by the Science Center of the National Science Foundation of China (Grant No. 52088101), the National Basic Research of China (Grant Nos. 2018YFA0305704, 2017YFA0303601, 2017YFA0206300, 2019YFA0704904, and 2016YFA0300701), the Project for Innovative Research Team of National Natural Science Foundation of China (Project No. 11921004), the National Natural Science Foundation of China (Grant Nos. 11934016 and 51972335), the Strategic Priority Research Program (B) of the Chinese Academy of Sciences (XDB33030200) and the Key Program of the Chinese Academy of Sciences. The calculations were performed in the Milky Way #2 supercomputer system at the National Supercomputer Center of Guangzhou, Guangzhou, China.

Data availability

All data generated or analyzed during this study are included in this article and its supplementary information.

Author contributions

X Chen and J Zhang contributed equally to this work.

Conflict of interest

There are no conflicts to declare.

ORCID iDs

Xiaobing Chen https://orcid.org/0000-0003-4327-1209
Jine Zhang https://orcid.org/0000-0001-7949-3239
Banggui Liu https://orcid.org/0000-0002-6030-6680
Jirong Sun https://orcid.org/0000-0003-1238-8770

References

[1] Dagotto E 2005 Complexity in strongly correlated electronic systems *Science* **309** 257

[2] Zubko P, Gariglio S, Gabay M, Ghosez P and Triscone J-M 2011 Interface physics in complex oxide heterostructures *Annu. Rev. Condens. Matter Phys.* **2** 141

[3] Ohtomo A and Hwang H Y 2004 A high-mobility electron gas at the $LaAlO_3/SrTiO_3$ heterointerface *Nature* **427** 423

[4] Nakagawa N, Hwang H Y and Muller D A 2006 Why some interfaces cannot be sharp *Nat. Mater.* **5** 204

[5] Kwak Y *et al* 2021 Non-BCS-type superconductivity and critical thickness of $SrTiO_3/LaAlO_3/SrTiO_3$ trilayer interface system *Appl. Surf. Sci.* **565** 150495

[6] Liu Y *et al* 2021 Multi-channel AlGaN/GaN Schottky barrier diodes with a half through-hole *Mater. Sci. Semicond. Process.* **133** 105934

[7] Ben Shalom M, Ron A, Palevski A and Dagan Y 2010 Shubnikov–de Haas oscillations in $SrTiO_3/LaAlO_3$ interface *Phys. Rev. Lett.* **105** 206401

[8] Choe D *et al* 2019 Gate-tunable giant nonreciprocal charge transport in noncentrosymmetric oxide interfaces *Nat. Commun.* **10** 4510

[9] Reyren N *et al* 2017 Superconducting interfaces between insulating oxides *Science* **317** 1196

[10] Brinkman A *et al* 2007 Magnetic effects at the interface between non-magnetic oxides *Nat. Mater.* **6** 493

[11] Chen Y Z *et al* 2013 A high-mobility two-dimensional electron gas at the spinel/perovskite interface of γ-$Al_2O_3/SrTiO_3$ *Nat. Commun.* **4** 1371

[12] Zhang H *et al* 2018 High-mobility spin-polarized two-dimensional electron gases at EuO/$KTaO_3$ interfaces *Phys. Rev. Lett.* **121** 116803

[13] He R *et al* 2020 Polarity-induced electronic and atomic reconstruction at $NdNiO_2$/$SrTiO_3$ interfaces *Phys. Rev.* B **102** 035118

[14] Geisler B and Pentcheva R 2020 Fundamental difference in the electronic reconstruction of infinite-layer versus perovskite neodymium nickelate films on $SrTiO_3$ (001) *Phys. Rev.* B **102** 020502(R)

[15] Tokura Y, Koshihara S, Arima T, Takagi H, Ishibashi S, Ido T and Uchida S 1990 Cu–O network dependence of optical charge-transfer gaps and spin-pair excitations in single-CuO_2-layer compounds *Phys. Rev.* B **41** 11657

[16] Takano M, Takeda Y, Okada H, Miyamoto M and Kusaka T 1989 $ACuO_2$ (A: alkaline earth) crystallizing in a layered structure *Physica* C **159** 375

[17] Kresse G and Furthmüller J 1996 Efficient iterative schemes for *ab initio* total-energy calculations using a plane-wave basis set *Phys. Rev.* B **54** 11169

[18] Kresse G and Joubert D 1999 From ultrasoft pseudopotentials to the projector augmented-wave method *Phys. Rev.* B **59** 1758

[19] Perdew J P, Burke K and Ernzerhof M 1996 Generalized gradient approximation made simple *Phys. Rev. Lett.* **77** 3865

[20] Perdew J P, Ruzsinszky A, Csonka G I, Vydrov O A, Scuseria G E, Constantin L A, Zhou X and Burke K 2008 Restoring the density-gradient expansion for exchange in solids and surfaces *Phys. Rev. Lett.* **100** 136406

[21] Monkhorst H J and Pack J D 1976 Special points for Brillouin-zone integrations *Phys. Rev.* B **13** 5188

[22] Dudarev S L, Botton G A, Savrasov S Y, Humphreys C J and Sutton A P 1998 Electron-energy-loss spectra and the structural stability of nickel oxide: an LSDA $+ U$ study *Phys. Rev.* B **57** 1505

[23] Okamoto S, Millis A J and Spaldin N A 2006 Lattice relaxation in oxide heterostructures: $LaTiO_3$/$SrTiO_3$ superlattices *Phys. Rev. Lett.* **97** 056802

[24] Anisimov V I, Zaanen J and Andersen O K 1991 Band theory and Mott insulators: Hubbard U instead of stoner I *Phys. Rev.* B **44** 943

[25] See supplemental materials for details about bulk properties of parent compounds, the convergence tests for computational details, plane-averaged electrostatic potential, orbital-resolved PDOS and orbital-projected band structures of interface Cu and surface O atom.

[26] Neugebauer J and Scheffler M 1992 Adsorbate-substrate and adsorbate–adsorbate interactions of Na and K adlayers on Al(111) *Phys. Rev.* B **46** 16067

[27] Popovic Z S, Satpathy S and Martin R M 2008 Origin of the two-dimensional electron gas carrier density at the $LaAlO_3$ on $SrTiO_3$ interface *Phys. Rev. Lett.* **101** 256801

[28] Santander-Syro A F *et al* 2011 Two-dimensional electron gas with universal subbands at the surface of $SrTiO_3$ *Nature* **469** 189

[29] Goniakowski J, Finocchi F and Noguera C 2008 Polarity of oxide surfaces and nanostructures *Rep. Prog. Phys.* **71** 016501

[30] Bristowe N C, Artacho E and Littlewood P B 2009 Oxide superlattices with alternating p and n interfaces *Phys. Rev.* B **80** 045425

[31] Pentcheva R and Pickett W E 2009 Avoiding the polarization catastrophe in $LaAlO_3$ overlayers on $SrTiO_3$ (001) through polar distortion *Phys. Rev. Lett.* **102** 107602

[32] Zhong Z, Koster G and Kelly P J 2012 Prediction of thickness limits of ideal polar ultrathin films *Phys. Rev.* B **85** 121411(R)

[33] Wang Y, Tang W, Cheng J, Behtash M and Yang K 2016 Creating two-dimensional electron gas in polar/polar perovskite oxide heterostructures: first-principles characterization of $LaAlO_3$/$A^+B^{5+}O_3$ *ACS Appl. Mater. Interfaces* **8** 13659

[34] Meevasana W, King P D C, He R H, Mo S-K, Hashimoto M, Tamai A, Songsiririthigul P, Baumberger F and Shen Z-X 2011 Creation and control of a two-dimensional electron liquid at the bare $SrTiO_3$ surface *Nat. Mater.* **10** 114

[35] Zhong Z, Tóth A and Held K 2013 Theory of spin–orbit coupling at $LaAlO_3$/$SrTiO_3$ interfaces and $SrTiO_3$ surfaces *Phys. Rev.* B **87** 161102(R)

[36] Overton T, Armstrong F A, Weller M and Rourke J 2018 *Inorganic Chemistry* vol 2 (Oxford: Oxford University Press) chapter 20 p 571

[37] Joshua A, Pecker S, Ruhman J, Altman E and Ilani S 2012 A universal critical density underlying the physics of electrons at the $LaAlO_3$/$SrTiO_3$ interface *Nat. Commun.* **3** 1129

[38] Gan Y *et al* 2019 Diluted oxide interfaces with tunable ground states *Adv. Mater.* **31** 1805970